

# Soluble Metal-Nanoparticle-Decorated Porous Coordination Polymers for the Homogenization of Heterogeneous Catalysis

Yuan-Biao Huang, Qiang Wang, Jun Liang, Xusheng Wang, and Rong Cao\*

State Key Laboratory of Structural Chemistry, Fujian Institute of Research on the Structure of Matter, Chinese Academy of Sciences, 155 Yangqiao Road West, 331800 Fuzhou, China

**S** Supporting Information

**ABSTRACT:** Ultrasmall metal nanoparticles (MNPs) were decorated on soluble porous coordination polymers (PCPs) with high metal loadings. The solubility of the composite and the size of the MNPs can be controlled by varying the ratio of the precursors to the supports. The soluble PCPs can serve as a platform to homogenize heterogeneous MNPs catalysts, which exhibited excellent activity and recyclability in C–H activation and Suzuki reactions. This strategy combines the advantages of homogeneous and heterogeneous catalysis and may bring new inspiration to catalysis.

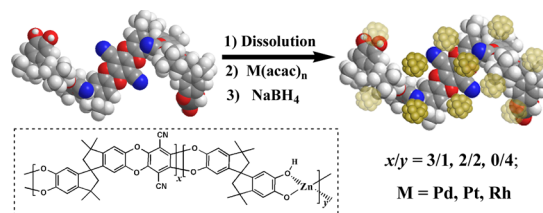
Homogeneous catalysts, in which the phase is the same as that of the reactants and all the active sites are accessible to the reactants in solution, often show higher activity than their heterogeneous counterparts but are difficult to recover and reuse.<sup>1</sup> Although heterogeneous catalysts such as supported metal nanoparticles (MNPs) lack this drawback, substrates cannot effectively contact with the active sites, which usually leads to lower activity.<sup>2</sup> The homogenization of heterogeneous MNPs catalysts is an alternative strategy to circumvent this drawback that combines the merits of homogeneous and heterogeneous catalysis to retain high activity and allow the recovery and reuse of the catalysts.<sup>3</sup> However, this promising approach has rarely been employed in catalysis systems consisting of MNPs supported on porous materials.<sup>4</sup> Although surfactant-stabilized MNPs can be easily dispersed in solution, the particles are covered with long chains, which usually restrict the free access of substrates to the catalytic MNPs.<sup>5</sup> MNPs supported on soluble porous materials with high dispersion ability can overcome this drawback because the MNPs are highly accessible to substrates through the channels.<sup>4a</sup>

Over the past few years, MNPs immobilized on metal–organic frameworks or porous coordination polymers (PCPs) have emerged as promising materials for catalysis due to their high surface areas, tunable cavities, and functionalities.<sup>6–11</sup> However, most PCPs have been restricted to microporous regimes, which usually makes the incorporation MNPs into the pores difficult and hampers the diffusion of large substrates to the active sites in solution.<sup>6c</sup> Thus, the synthesis of ultrasmall MNPs supported on PCPs is another challenge to improve the activity because of the high surface area-to-volume ratio of the particles.<sup>6–9</sup> Moreover, most PCPs are insoluble in common solvents, which usually results in the poor dispersion of MNPs and low metal loading. Therefore, developing a facile and

general approach to prepare soluble PCP-supported ultrasmall MNPs for enhanced catalysis is highly desirable.

Soluble PCPs based on the highly contorted and rigid ligand 5,5',6,6'-tetrahydroxy-3,3,3',3'-tetramethyl-1,1'-spirobisindane, tetrafluoroterephthalonitrile (TFTPN), and Zn(OAc)<sub>2</sub> were easily prepared by a known mechanochemical method.<sup>12</sup> The presence of cyano groups on TFTPN ligands may offer facile stabilization of ultrasmall MNPs,<sup>13</sup> and the contorted shape and the rigidity of the ligands can induce intrinsic microporous PCPs to facilitate the accessibility of substrates to ultrasmall MNPs.<sup>14</sup> Hence, the corresponding PCPs were prepared and denoted as SPCP-*x/y* (*x/y* = 3/1, 2/2, and 0/4), where *x/y* is the molar ratio of TFTPN and Zn(OAc)<sub>2</sub>. Among the SPCPs, SPCP-3/1 is soluble in polar solvents and we hope it can stabilize ultrasmall MNPs and serve as a platform for the homogenization of heterogeneous catalysis. As expected, ultrasmall MNPs supported on SPCP-3/1 (M@SPCP-3/1, M = Pd, Pt, and Rh) were readily prepared and produced a solution (Scheme 1). Such soluble catalysts have several

**Scheme 1. Synthesis of Ultrasmall MNPs Immobilized on Porous SPCP-*x/y* (*x/y* = 3/1, 2/2, and 0/4)**



remarkable features, including (1) effective control over ultrasmall MNPs at very high loadings, (2) high stability and dispersity in solution, (3) significant enhancement of the efficiency of liquid-phase reactions, and (4) excellent recycling and reusability.

SPCP-3/1 is insoluble in nonpolar solvents such as hexane and ethyl ether but can dissolve in solvents such as DMF, CH<sub>2</sub>Cl<sub>2</sub>, and 1,4-dioxane. In contrast, SPCP-2/2 only partially dissolved in polar solvents, while SPCP-0/4 only dissolved in acetic acid.<sup>12</sup> The N<sub>2</sub> sorption measurements showed that SPCP-3/1 had the highest N<sub>2</sub> uptake among the three samples with a Brunner–Emmett–Teller (BET) surface area of 331 m<sup>2</sup> g<sup>-1</sup> (Figure S1a) and indeed had an intrinsic microporous

Received: June 15, 2016

Published: August 3, 2016

characteristic.<sup>14</sup> Furthermore, remarkable hysteresis loops at  $P/P^0 = 0.45-0.9$  were observed in all the samples, which indicates that meso-/macropores were formed by interstitial voids (Figure S1).

Pd NPs-decorated SPCP-3/1 (denoted as Pd@SPCP-3/1) was prepared by the addition of palladium acetylacetonate, followed by reduction with  $\text{NaBH}_4$  (Scheme 1). Transmission electron microscopy (TEM), high-angle annular dark-field scanning TEM (HAADF-STEM), and high-resolution TEM (HRTEM) revealed that the ultrasmall Pd NPs were uniformly distributed on SPCP-3/1 (2.61 wt% Pd) with a narrow size distribution of  $(1.5 \pm 0.3)$  nm (Figures 1a,c and S2). X-ray

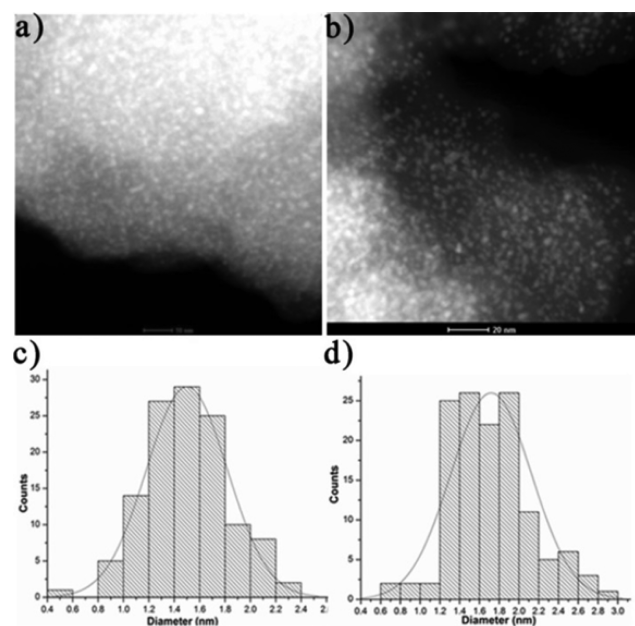


**Figure 1.** HAADF-STEM images of Pd@SPCP-3/1 and size histograms of the corresponding Pd NPs: (a) 2.61 wt% Pd loading, (b) 9.91 wt% Pd loading, (c)  $(1.5 \pm 0.3)$  nm size distribution, and (d)  $(1.7 \pm 0.4)$  nm size distribution. Scale bars represent 10 nm in (a) and 20 nm in (b).

photoelectron spectroscopy (XPS) revealed that the peaks at 335.9 and 341.3 eV correspond to Pd  $3d_{5/2}$  and Pd  $3d_{3/2}$ , respectively (Figure S3), which also identifies the formation of the  $\text{Pd}^0$ .<sup>15</sup> Interestingly, Pd@SPCP-3/1 (2.61 wt% Pd) was soluble in  $\text{CH}_2\text{Cl}_2$ , DMF, and 1,4-dioxane, which is ascribed to the ultrasmall NPs and the soluble SPCP-3/1. Compared with SPCP-3/1, Pd@SPCP-3/1 (2.61 wt% Pd) had a lower BET surface area ( $117 \text{ m}^2 \text{ g}^{-1}$ , Figure S1, Table S1), indicating that partial pores of SPCP-3/1 were blocked by the Pd NPs.<sup>9</sup> Nevertheless, the presence of hysteresis loops in the  $\text{N}_2$  isotherms indicates that the mesopores remained after the NPs were loaded, which will facilitate the diffusion of the reactants to the active sites.<sup>7c</sup>

The size of the Pd NPs on SPCP-3/1 could be effectively controlled by varying the loading amount of the precursors. When the Pd loading amount was increased to 9.91 wt%, ultrasmall Pd NPs with an average diameter of  $(1.7 \pm 0.4)$  nm were obtained (Figures 1b,d, S4, and S5). Notably, a high loading of MNPs of such a small size was difficult to obtain in other PCP-supported MNPs.<sup>6</sup> Pd@SPCP-3/1 (9.91 wt% Pd) only partially dissolved in  $\text{CH}_2\text{Cl}_2$ , DMF, and 1,4-dioxane due to the high concentration of Pd NPs. Interestingly, when the Pd

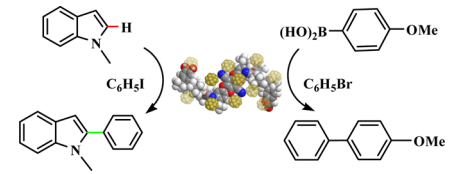
loading amount was increased beyond 19.11 wt%, uniform Pd NPs with small size distributions (ca. 3 nm) were also observed, even with a loading of 78.50 wt% Pd (Figures S6–S8).

Ultrafine Pd NPs supported on SPCP-2/2 with an average size of  $(1.7 \pm 0.3)$  nm were also formed (Figure S9). In contrast, the size of the Pd NPs embedded in SPCP-0/4 increased to  $(3.5 \pm 0.8)$  nm because the support was insoluble in  $\text{CH}_2\text{Cl}_2$  and there was no cyano group to stabilize the NPs (Figure S10). In comparison, Pd NPs stabilized by polyvinylpyrrolidone (PVP) produced large NPs with an average diameter of  $(4.8 \pm 1.3)$  nm (Figure S11). Unsurprisingly, large black Pd aggregates (Pd-SP-free) formed in the absence of a stabilizer (Figure S12).

Other ultrafine MNPs can also be decorated on SPCPs. For example, tiny Pt and Rh NPs were well dispersed on SPCP-3/1 with size distribution of  $(1.5 \pm 0.3)$  and  $(0.7 \pm 0.1)$  nm, respectively (Figures S13 and S14). Interestingly, the Rh NPs at a loading of nearly 10 wt% can dissolve in  $\text{CH}_2\text{Cl}_2$  due to the ultrasmall size. The results indicate that the soluble SPCP-3/1 provides a powerful platform for the growth of ultrasmall MNPs.

C–H activation<sup>16,17</sup> was studied to illustrate the superiority of the homogenization of heterogeneous SPCP-decorated MNPs catalysts. We explored the behavior of Pd@SPCPs in the direct C–H arylation of *N*-methylindole with aryl halides. As shown in Table 1, the activity was highly dependent on the solubility of the catalysts. Although the catalysts Pd@SPCP-3/1 (2.61 wt% Pd), Pd@SPCP-3/1 (9.91 wt% Pd), and Pd/SPCP-2/2 (2.41 wt% Pd) have Pd NPs of similar sizes, the soluble catalyst Pd@SPCP-3/1 (2.61 wt% Pd) showed the highest activity under the same conditions, with 86% yield of the C2-arylation product (Table 1, entries 1–3). Furthermore, large substrates such as 1-iodonaphthalene also gave satisfactory activity (Table S2). The high activity of Pd@SPCP-3/1 (2.61 wt% Pd) can be reasonably attributed to the soluble ultrasmall Pd NPs with highly accessible active sites in solution, which are favorable for contact between the reactants and Pd NPs. The latter two catalysts exhibited moderate activity due to their partial dissolution, reducing the contact with the reactants. Unsurprisingly, the insoluble catalysts, Pd@SPCP-3/1 with high Pd loading amounts (19.11, 49.87, and 78.50 wt% Pd) and Pd/SPCP-0/4 (2.51 wt% Pd), resulted in poor yields (Table 1, entries 4–7), although the effect of Pd NPs of a larger size cannot be excluded. In addition, Pd@SPCP-3/1 (2.61 wt% Pd) required only 12 h to attain high yields when using aryl iodides (Table 1, entry 1, and Table S2) and enhanced yields when using bromobenzene and chlorobenzene (Table S3). In contrast, Pd NPs encapsulated in the mesopores of MIL-101 required much more time to complete the same reaction due to the slow diffusion of reactants to access the insoluble catalytic active sites.<sup>18</sup> More importantly, compared with other homogeneous catalysts such as  $\text{Pd}(\text{OAc})_2$ , which requires at least 0.5 mol% Pd and 24 h reaction time, the lower required amount of our catalyst (0.1 mol% Pd) and shorter time highlight the advantages of using a soluble catalyst in the homogenization of heterogeneous SPCP-stabilized MNPs to improve catalytic performance.<sup>17</sup>

Furthermore, although the conventional catalyst Pd/PVP is soluble in DMF, it showed very poor activity (Table 1, entry 8, and Tables S2 and S3). The active sites in Pd/PVP were blocked by the long alkyl chains of PVP, which led to slow kinetics. The control experiments demonstrate that the high solubility and the cyano groups of SPCP-3/1 endow the MNPs

**Table 1. Results for the C–H Arylation of Indole<sup>a</sup> and Suzuki Reaction<sup>b</sup> Catalyzed by Pd Catalysts**


entry	catalyst	solubility <sup>c</sup>	size (nm) <sup>d</sup>	yield (%) <sup>e</sup>	
				C–H activation	Suzuki reaction
1	Pd@SPCP-3/1 (2.61 wt% Pd)	D <sup>f</sup>	1.5 ± 0.3	86	89
2	Pd@SPCP-3/1 (9.91 wt% Pd)	PD <sup>g</sup>	1.7 ± 0.4	68	64
3	Pd@SPCP-2/2 (2.41 wt% Pd)	PD <sup>h</sup>	1.7 ± 0.3	67	62
4	Pd@SPCP-3/1 (19.11 wt% Pd)	ND	3.4 ± 0.6	49	59
5	Pd@SPCP-3/1 (49.87 wt% Pd)	ND	3.1 ± 0.5	46	48
6	Pd@SPCP-3/1 (78.50 wt% Pd)	ND	3.1 ± 0.8	37	39
7	Pd@SPCP-0/4 (2.51 wt% Pd)	ND	3.5 ± 0.8	33	41
8	Pd/PVP	D	4.8 ± 1.3	21	37
9	Pd-SP-free	ND	aggregate	trace	trace

<sup>a</sup>Conditions: *N*-methylindole (1 mmol), iodobenzene (1.2 mmol), 0.1 mol% Pd based on *N*-methylindole, CsOAc (2 mmol), DMF (1 mL), 120 °C, *t* = 12 h, under air. <sup>b</sup>Conditions: bromobenzene (1 mmol), 4-methoxyphenylboronic acid (1.2 mmol), 0.1 mol% Pd based on bromobenzene, K<sub>3</sub>PO<sub>4</sub>·3H<sub>2</sub>O (1.2 mmol), 1,4-dioxane/H<sub>2</sub>O (3/0.5 mL), 40 °C, *t* = 3 h. <sup>c</sup>Solubility was tested in DMF and 1,4-dioxane: D = dissolved, PD = partially dissolved, and ND = not dissolved (see Supporting Information). <sup>d</sup>Determined by TEM. <sup>e</sup>GC yield. <sup>f</sup>Concentration was ca. 4 mg/mL. <sup>g</sup>Dissolved concentration was ca. 0.4 and 0.3 mg/mL in DMF and 1,4-dioxane, respectively. <sup>h</sup>Dissolved concentration was ca. 0.4 and 0.2 mg/mL in DMF and 1,4-dioxane, respectively.

with good dispersibility and prevent the MNPs from aggregating (Figures S15 and S16). In particular, the soluble SPCP-3/1 with hierarchical porosity favors the accessibility of substrates to the active sites and is superior to the nonporous surfactant stabilizer.

The unique features of SPCP-3/1 could boost the kinetics of the liquid-phase catalytic process, which was also verified by Suzuki reaction.<sup>19</sup> As expected, Pd@SPCP-3/1 (2.61 wt% Pd) gave the best yield (Table 1, entry 1); even for large aryl bromides such as 9-bromoanthracene, 2-bromonaphthalene, and 5'-bromo-*m*-terphenyl, high yields were also obtained (Table S4). In contrast, the insoluble catalysts showed lower activity under similar conditions (Table 1, entries 2–9). This enhanced activity further indicates that the homogenization of heterogeneous catalysts is a general method that improves the efficiency of reactions.

The soluble Pd@SPCP-3/1 (2.61 wt% Pd) could be recovered and reused. The C–H activation and Suzuki reaction were performed to verify the recyclability and reusability of Pd@SPCP-3/1 (2.61 wt% Pd). After completion of the reaction and addition of low-polarity solvents, the catalyst was readily recovered. After three cycles, the high yields of the reactions were maintained (Figures S17 and S18). TEM revealed that the sizes of the Pd NPs increased slightly compared with those before the reactions (Figures S19 and

S20). The XPS spectrum demonstrated that only a small part of Pd was oxidized (Figure S21). ICP analysis showed that the amount of Pd in the filtrate was negligible, and only 0.528 and 0.83 ppm for Suzuki reaction and C–H activation was detected, respectively. These investigations further demonstrate that Pd@SPCP-3/1 (2.61 wt% Pd) possesses several advantages in homogeneous and heterogeneous catalysis: high activity, recyclability, and reusability.

In summary, we have developed a facile method to prepare highly dispersible, stable, and ultrasmall MNPs immobilized on soluble PCPs at high loadings. Illustrating the catalytic applications, the soluble Pd@SPCP-3/1 (2.61 wt% Pd) exhibited superior catalytic performances in C–H activation and Suzuki reactions, demonstrating higher activity than the heterogeneous counterparts. Moreover, this soluble catalyst showed high stability and could be recovered and reused. With such unique properties of the porous soluble catalyst, the strategy may bring new inspiration to catalysis by combining the advantages of both homo- and heterogeneous catalysis.

## ■ ASSOCIATED CONTENT

### 📄 Supporting Information

The Supporting Information is available free of charge on the ACS Publications website at DOI: 10.1021/jacs.6b06185.

Experimental details, adsorption studies, TEM images, and XPS and other spectra, including Tables S1–S4 and Figures S1–S21 (PDF)

## ■ AUTHOR INFORMATION

### Corresponding Author

\*rcao@fjirsm.ac.cn

### Notes

The authors declare no competing financial interest.

## ■ ACKNOWLEDGMENTS

We acknowledge financial support from the 973 Program (2014CB845605 and 2013CB933200), NSFC (21521061, 21331006, and 21273238), Strategic Priority Research Program of the Chinese Academy of Sciences (XDB20000000), Youth Innovation Promotion Association, CAS (2014265), and Chunmiao Project of the Haixi Institute of the Chinese Academy of Sciences (CMZX-2014-004).

## ■ REFERENCES

- (1) Phan, N. T. S.; van der Sluys, M.; Jones, C. W. *Adv. Synth. Catal.* **2006**, *348*, 609.
- (2) Dhakshinamoorthy, A.; Asiri, A. M.; Garcia, H. *Chem. Soc. Rev.* **2015**, *44*, 1922.
- (3) de Almeida, M. P.; Carabineiro, S. A. C. *ChemCatChem* **2012**, *4*, 18.
- (4) (a) Sun, J. K.; Zhan, W. W.; Akita, T.; Xu, Q. *J. Am. Chem. Soc.* **2015**, *137*, 7063. (b) Witham, C. A.; Huang, W.; Tsung, C. K.; Kuhn, J. N.; Somorjai, G. A.; Toste, F. D. *Nat. Chem.* **2010**, *2*, 36. (c) Huang, W.; Liu, J. H. C.; Alayoglu, P.; Li, Y.; Witham, C. A.; Tsung, C. K.; Toste, F. D.; Somorjai, G. A. *J. Am. Chem. Soc.* **2010**, *132*, 16771.
- (5) Niu, Z.; Li, Y. *Chem. Mater.* **2014**, *26*, 72.
- (6) (a) Falcaro, P.; Ricco, R.; Yazdi, A.; Imaz, I.; Furukawa, S.; Maspocho, D.; Ameloot, R.; Evans, J. D.; Doonan, C. J. *Coord. Chem. Rev.* **2016**, *307*, 237. (b) Zhu, Q. L.; Xu, Q. *Chem. Soc. Rev.* **2014**, *43*, 5468. (c) Moon, H. R.; Lim, D. W.; Suh, M. P. *Chem. Soc. Rev.* **2013**, *42*, 1807. (d) Dhakshinamoorthy, A.; Garcia, H. *Chem. Soc. Rev.* **2012**, *41*, 5262. (e) Hu, P.; Morabito, J. V.; Tsung, C. K. *ACS Catal.* **2014**, *4*, 4409.

(7) (a) Choi, K. M.; Na, K.; Somorjai, G. A.; Yaghi, O. M. *J. Am. Chem. Soc.* **2015**, *137*, 7810. (b) Liu, X.; He, L.; Zheng, J.; Guo, J.; Bi, F.; Ma, X.; Zhao, K.; Liu, Y.; Song, R.; Tang, Z. *Adv. Mater.* **2015**, *27*, 3273. (c) Khajavi, H.; Stil, H. A.; Kuipers, H. P. C. E.; Gascon, J.; Kapteijn, F. *ACS Catal.* **2013**, *3*, 2617.

(8) (a) Zhao, Y.; Kornienko, N.; Liu, Z.; Zhu, C.; Asahina, S.; Kuo, T.; Bao, W.; Xie, C.; Hexemer, A.; Terasaki, O.; Yang, P.; Yaghi, O. M. *J. Am. Chem. Soc.* **2015**, *137*, 2199. (b) Pascanu, V.; Carson, F.; Solano, M. V.; Su, J.; Zou, X.; Johansson, M. J.; Martin-Matute, B. *Chem. - Eur. J.* **2016**, *22*, 3729. (c) Lu, G.; Li, S.; Guo, Z.; Farha, O. K.; Hauser, B. G.; Qi, X.; Wang, Y.; Wang, X.; Han, S.; Liu, X.; DuChene, J. S.; Zhang, H.; Zhang, Q.; Chen, X.; Ma, J.; Loo, S. C. J.; Wei, W. D.; Yang, Y.; Hupp, J. T.; Huo, F. *Nat. Chem.* **2012**, *4*, 310.

(9) Guo, Z.; Xiao, C.; Maligal-Ganesh, R. V.; Zhou, L.; Goh, T. W.; Li, X.; Tesfagaber, D.; Thiel, A.; Huang, W. *ACS Catal.* **2014**, *4*, 1340.

(10) (a) Wang, C.; deKrafft, K. E.; Lin, W. *J. Am. Chem. Soc.* **2012**, *134*, 7211. (b) Hermes, S.; Schröter, M. K.; Schmid, R.; Khodeir, L.; Muhler, M.; Tissler, A.; Fischer, R. W.; Fischer, R. A. *Angew. Chem., Int. Ed.* **2005**, *44*, 6237. (c) Liu, H.; Chang, L.; Bai, C.; Chen, L.; Luque, R.; Li, Y. *Angew. Chem., Int. Ed.* **2016**, *55*, 5019. (d) Li, G.; Kobayashi, H.; Taylor, J. M.; Ikeda, R.; Kubota, Y.; Kato, K.; Takata, M.; Yamamoto, T.; Toh, S.; Matsumura, S.; Kitagawa, H. *Nat. Mater.* **2014**, *13*, 802.

(11) (a) Furukawa, S.; Reboul, J.; Diring, S.; Sumida, K.; Kitagawa, S. *Chem. Soc. Rev.* **2014**, *43*, 5700. (b) Li, J. R.; Sculley, J.; Zhou, H. C. *Chem. Rev.* **2012**, *112*, 869.

(12) Zhang, P.; Li, H.; Veith, G. M.; Dai, S. *Adv. Mater.* **2015**, *27*, 234.

(13) Maurin-Pasturel, G.; Long, J.; Guari, Y.; Godiard, F.; Willinger, M.; Guerin, C.; Larionova, J. *Angew. Chem., Int. Ed.* **2014**, *53*, 3872.

(14) Carta, M.; Malpass-Evans, R.; Croad, M.; Rogan, Y.; Jansen, J. C.; Bernardo, P.; Bazzarelli, F.; McKeown, N. B. *Science* **2013**, *339*, 303.

(15) Yun, G.; Hassan, Z.; Lee, J.; Kim, J.; Lee, N. S.; Kim, N. H.; Baek, K.; Hwang, I.; Park, C. G.; Kim, K. *Angew. Chem., Int. Ed.* **2014**, *53*, 6414.

(16) (a) Tang, R. Y.; Li, G.; Yu, J. Q. *Nature* **2014**, *507*, 215. (b) Stuart, D. R.; Fagnou, K. *Science* **2007**, *316*, 1172.

(17) Platon, M.; Amardeil, R.; Djakovitch, L.; Hierso, J. C. *Chem. Soc. Rev.* **2012**, *41*, 3929.

(18) Huang, Y.; Lin, Z.; Cao, R. *Chem. - Eur. J.* **2011**, *17*, 12706.

(19) Fihri, A.; Bouhrara, M.; Nekoueishahraki, B.; Basset, J. M.; Polshettiwar, V. *Chem. Soc. Rev.* **2011**, *40*, 5181.